Phase diagram of the hexagonal lattice quantum dimer model

R. Moessner,[1] S. L. Sondhi,[1] and P. Chandra[2]
[1]*Department of Physics, Jadwin Hall, Princeton University, Princeton, New Jersey 08544*
[2]*NEC Research Institute, 4 Independence Way, Princeton, New Jersey 08540*
(Received 22 March 2001; published 19 September 2001)

We discuss the phase diagram of the quantum dimer model on the hexagonal (honeycomb) lattice. In addition to the columnar and staggered valence-bond solids which have been discussed in previous work, we establish the existence of a plaquette valence-bond solid. The transition between the plaquette and columnar phases at $v/t=-0.2\pm0.05$ is argued to be first order. We note that this model should describe valence-bond-dominated phases of frustrated Heisenberg models on the hexagonal lattice and discuss its relation to recent exact diagonalization work by Fouet *et al.* on the J_1-J_2 model on the same lattice. Our results also shed light on the properties of the transverse field Ising antiferromagnet on the triangular lattice and the classical Ising antiferromagnet on the stacked triangular lattice, which are related to dimer models by duality.

DOI: 10.1103/PhysRevB.64.144416 PACS number(s): 75.10.Jm, 05.50.+q, 05.30.−d

I. INTRODUCTION

Quantum dimer models (QDM's) were introduced to describe the physics of Heisenberg antiferromagnets in a regime dominated by valence bonds.[1] This regime is best realized in cases where the conventional Néel state is destabilized by quantum fluctuations or prohibited by frustration. The most prominent appearance of such dimer models has been in the context of the superconductivity of the cuprates, where the QDM on the square lattice was introduced by Rokhsar and Kivelson[1] (RK) to describe the physics of the short-range flavor[2] of resonating valence bond (RVB) physics.[3] Subsequently, Read and Sachdev showed that QDM's arise naturally in certain ''extreme quantum limits'' of generalizations of SU(2) magnets to SU(N) or Sp(N) symmetry with large N.[4]

More recently, an exact duality between QDM's in $d=2$ and frustrated Ising models in a weak transverse field was explored by the present authors.[5] This mapping connects the QDM not only to transverse field Ising models but also to a class of ferromagnetically stacked frustrated Ising magnets in dimension $d=2+1$, which are of independent interest as they also have a range of experimental realizations.[6] The connection between QDM's, short-ranged RVB physics, and Ising gauge theories has also been discussed recently by Fradkin and two of the present authors (R.M. and S.L.S.).[7]

From the work to date, it appears that the QDM on the square lattice does not realize the disordered phase envisaged in the short-ranged RVB scenario of high-temperature superconductivity. Rather, it is ordered everywhere except at a point, a possibility already noted in RK's original work[1] and fleshed out from various viewpoints by different authors.[8–10,4,11,12,5] While some evidence has been presented dissenting from this scenario,[13,11] as will become clear in the following, we believe there no longer is any real basis for doubting it.

The physics of the square lattice QDM is closely connected to the physics of the hexagonal lattice QDM—both lattices exhibit critical classical dimer correlations which can be traced, via height representations, to their bipartite nature. (In contrast the nonbipartite triangular lattice exhibits disordered classical correlations and an RVB phase in its QDM.[14]) This connection was discussed first by Read and Sachdev (see Ref. 4) and has more recently been discussed by us in the context of a study of frustrated transverse field Ising models.[5]

Whereas the general structure of the phase diagram for both problems has been in place for some time, settling the detailed structure has turned out to be difficult. Approaches based on mappings to height models or Landau-Ginzburg-Wilson theory contain undetermined parameters upon which the detailed nature of the ordering pattern depends. From the point of view of numerics, the problems of simulating the quantum problem have been restrictive in that the studies thus far have been limited to diagonalizations of systems of rather small size,[8,11] from which subtle differences in correlations have been difficult to read off.

In this paper, we solve this problem for the the QDM on the hexagonal (honeycomb) lattice and map out its phase diagram. This is done with the aid of the above-mentioned mapping to a *classical* stacked triangular Ising magnet. This mapping gives access to a number of analytical results but, more importantly, allows efficient numerical simulations of systems much larger than the ones previously studied.

Our central result is that the QDM on the hexagonal lattice has three phases, namely, a staggered, a plaquette, and a columnar valence-bond solid (VBS). The transitions between these phases are a first-order transition between the columnar and plaquette phases and a combination of a first-order and continuous transition in the case of the plaquette and staggered phases; the latter involves fluctations in the ground state on one side of the transition but not on the other.

We further discuss the implications of these results for the properties of stacked triangular Ising magnets with nearest-neighbor interactions,[15–22,6] for which our algorithm allows us to avoid some numerical limitations encountered in previous studies and where extension to the QDM provides considerable insight into the stability of the low-temperature phase. This phase turns out to be one with three inequivalent sublattices, one of which is disordered, in accordance with the results of some, but not all, previous studies.

We also review the connection of the QDM under study to

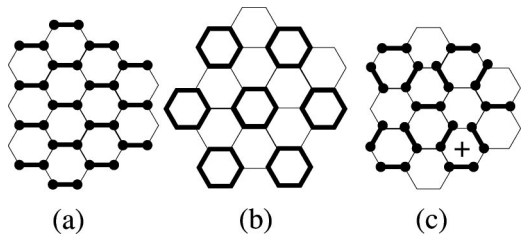

FIG. 1. Dimer patterns on the hexagonal lattice: (a) staggered, (b) plaquette, and (c) columnar. The marked links have a high probability of being occupied by a dimer in the respective phases. Note that in each case, there are only two inequivalent sets of links. A dimer plaquette move effected by $\hat{T}$ consists of rotating the three dimers surrounding a plaquette (like the one labeled with a plus) by 60°.

frustrated Heisenberg antiferromagnets on the hexagonal lattice. Such magnets are prime candidates for being described by the quantum dimer model, and it turns out that the Heisenberg model with competing interactions does indeed seem to realize the order present in two of the phases of the QDM.[23]

Turning to the QDM, its Hilbert space consists of hard-core dimer coverings of the hexagonal lattice. The Hamiltonian acts on each hexagonal plaquette of the lattice. It contains two terms, a kinetic ($\hat{T}$) and a potential ($\hat{V}$) one. The former generates a plaquette resonance move by rotating a triplet of dimers by 60° (see Fig. 1), in analogy to the benzene resonance.[24] The latter is diagonal in the dimer basis and simply counts the number of plaquettes able to resonate (''flippable plaquettes'').

The Hamiltonian of the QDM can thus be represented as a sum over plaquettes of the following plaquette Hamiltonian:

$$H_{QDM} = -t\hat{T} + v\hat{V} = -t\,(|\nabla\rangle\langle\Delta| + \text{H.c.}) + v\,(|\nabla\rangle\langle\nabla| + |\Delta\rangle\langle\Delta|). \tag{1}$$

It has one free parameter, namely, the ratio of the strength of the potential and kinetic terms, v/t.

The structure of this paper is as follows. In Sec. II, we discuss the phases which one might expect to encounter in the model under consideration. Section III contains a summary of the methods used to establish the results that follow. The numerical results on the QDM are presented in Sec. IV, from which the phase diagram (Sec. V) follows. We then discuss implications for the study of magnets, namely, triangular stacked Ising (Sec. VI) and $S=1/2$ hexagonal Heisenberg (Sec. VII) models. We close with a conclusion in Sec. VIII.

II. CANDIDATE PHASES

As mentioned above, the QDM on the hexagonal lattice is closely connected to its square lattice version. Hence a number of known exact statements on the square lattice carry over *mutatis mutandis* to the hexagonal lattice. First, for $v > t$, the ground state is the staggered state, $|\varphi\rangle$, depicted in Fig. 1(a). This follows from the fact that a lower bound on the energy per plaquette is $\min\{0, v-t\}$, and only $|\varphi\rangle$ saturates this bound for $v>t$, with $H_{QDM}|\varphi\rangle = 0$. The dimer configuration corresponding to $|\varphi\rangle$ turns out to constitute a topological sector of its own. (Two configurations belong to the same topological sector if one can be obtained from another by strictly local rearrangements of the dimers.[1])

As one decreases v through t, the ground state moves into another sector, which contains an exponentially large number of dimer configurations. The two candidate phases in this sector are depicted in Figs. 1(b) and 1(c); these are the plaquette and columnar valence-bond solids, respectively. In fact, for $v/t \to -\infty$, one can see that the ground state will be the columnar state, as this maximizes the number of flippable plaquettes favored by the potential term.

The point $v/t=1$ is the RK point where each equal-amplitude superposition over a winding number sector is a ground state. An analysis in terms of height representations[25] shows that there is a diverging correlation length as one approaches this point from $v<t$ and that the critical theory is Gaussian. In the same language the two candidate states mentioned above for $v<t$ are flat but the competition between them cannot be settled in the same analysis. We now turn to an alternative mapping of the physics of the QDM which will allow us to settle that question by computation.

III. USEFUL MAPPINGS AND NUMERICAL METHOD

This alternative, duality, mapping crisply distinguishes between the different phases. This mapping takes the QDM in $d=2$ onto a classical, stacked, frustrated, anisotropic Ising magnet in $d=2+1$ on its *dual* lattice.[5] The Hamiltonian for that model reads

$$\beta_C H_{Ising} = K^{\xi} \sum_{\langle ij \rangle} \sigma_i \sigma_j - K^{\tau} \sum_{\langle ii' \rangle} \sigma_i \sigma_{i'} + \beta_C v_C \sum_i \delta_{B_i,0}. \tag{2}$$

Here, the σ is the Ising variable defined on the sites of a stacked triangular lattice; the sum on $\langle ij \rangle$ runs over nearest-neighbor pairs in the plane, whereas the one on $\langle ii' \rangle$ is over pairs in adjacent layers. B_i is the in-plane exchange field experienced by spin i; if it is zero, the corresponding dimer plaquette is flippable.

To generate equivalent Hilbert spaces, one has to take the limit of infinite exchange in the planes, $K^{\xi} \to +\infty$, as there is a one-to-one correspondence between the hard-core dimer coverings on the hexagonal lattice and the Ising model ground states on the triangular lattice, up to a global spin reversal.[26]

The equivalence then holds in the scaling limit $K^{\tau} \to +\infty$, with the quantum inverse temperature β_Q given by $\beta_Q t = \exp(2K^{\tau})/N \equiv \lambda/N$, where N is the number of stacked layers, so that the zero-temperature limit corresponds to a system with infinite extent in the stacking direction. The conversion of parameters between the classical (C) and quantum (Q) problems proceeds via the formula $v_Q/t = \beta_C v_C \lambda$. In the following, the quoted values of v/t are to be understood as referring to the quantum problem. Note that λ (which we will quote in the following) quantifies the discretization

error—it gives a rough measure of a typical correlation length in the stacking direction.

For the case $v=0$, this model has been studied in the past by several groups. In an influential piece of work, Blankschtein and co-workers[15] have carried out a Landau-Ginzburg-Wilson (LGW) analysis for this model, which uncovered an XY-symmetric action with an (in $d=2+1$ dangerously irrelevant) sixfold clock term, which breaks the XY symmetry at sixth order.

The ordering pattern obtained by this method is a three-sublattice ordering pattern; depending on the sign of the sixfold clock term, the three sublattices have the ordering pattern $(+M,0,-M)$ or $(+m,-n,-n)$, where the amplitudes M, m, and n are undetermined in the most general scenario.[27] Translating these back to dimer correlations, one finds that the former pattern corresponds to the plaquette VBS, whereas the latter corresponds to the columnar VBS.

Simulating H_{Ising} is evidently straightforward in principle using classical Monte Carlo simulations in $d=3$. The only complication arises from the scaling limit which has to be taken, requiring long correlation lengths in the stacking direction. Here, we use a cluster algorithm,[28] the implementation of which is easy in Ising language, but would have been rather hard to guess at for simulations of a stacked dimer model. The mapping onto the stacked classical Ising model, together with the cluster algorithm, is what enables us to simulate system sizes which are substantially in excess of those treated so far in numerical studies of the QDM.

IV. NUMERICAL RESULTS

In this section, we display the results of our numerical simulations, which we argue demonstrate the existence of a phase transition from the columnar to the plaquette VBS around $v/t=-0.2\pm0.05$.

Since we know that the columnar phase is encountered in the limit $v/t\to-\infty$, we can rephrase the question of whether there also is the plaquette phase by asking whether there is a phase transition as v/t is increased towards $+1$. From the discussion in the previous section, it is apparent that, in spin language, the plaquette state has zero magnetization whereas the columnar state does not. All we therefore have to do is to look for restoration of the Ising symmetry to discover whether there exists a plaquette phase.

To give an impression of the general phase diagram, consider Fig. 2, where we plot the root-mean-square magnetization m_{rms} of the equivalent Ising model for small to moderate system sizes over a broad range of the parameter v/t. We quote system sizes in terms of number of sites. This is the number of unit cells of the hexagonal lattice, which equals the number of dimers and also the number of spins of the dual triangular lattice. From this plot, a number of important features are already visible.

First, for large $-v/t$, m_{rms} approaches its limiting value within the ground states of the Ising model, which is 1/3. Deviations are well captured perturbatively in t/v, as depicted by the dashed line, which shows the lowest-order result. Just to the left of $v/t=0$, one can witness the vanishing of m_{rms}, which gets sharper with increasing system size.

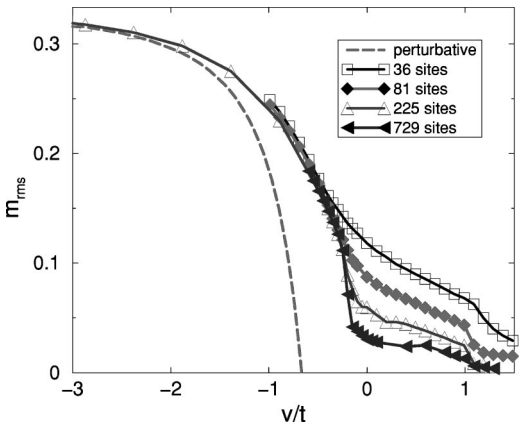

FIG. 2. m_{rms} as a function of v/t, in the sector containing the columnar and plaquette phases. In this sector, the actual transition at $v/t=1$ to a state with strictly zero m_{rms} shows up as a depression thereof. $\beta_Q t=0.083$, $\lambda=10$.

Finally, at the Rokhsar-Kivelson point $v/t=1$, there is a kink in m_{rms}, which indicates the further transition to the staggered state. The staggered state has strictly zero magnetization, but since it is in a different sector from the other two states, this shows up as a depression of m_{rms} as v is swept through t, as the system tries to accommodate local staggered correlations within the wrong topological sector as best it can.

To get a handle on the details of the transition, we examine the same plot for a much narrower range of v/t near the vanishing of m_{rms}, for a wider range of system sizes, as depicted in Fig. 3. As the system size increases, the transition sharpens up into a discontinuous drop in m_{rms}. This drop separates the region on the left, with m_{rms} decreasing with an almost constant slope, from that on the right, with m_{rms} being near constant and close to zero. The phase transition thus appears to be of first order, as will be discussed in more detail below.

To underline this result, we plot the scaling of m_{rms} as a function of inverse linear system size for a number of values of v/t near the transition in Fig. 4. This plot shows that m_{rms}

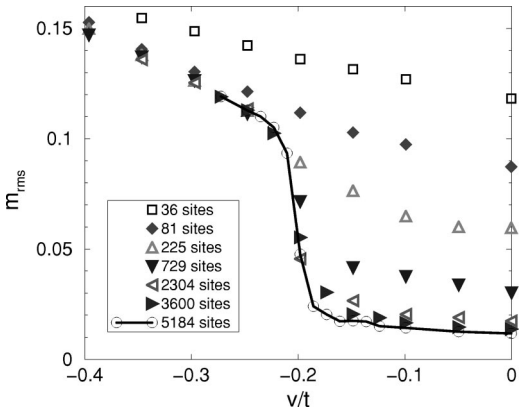

FIG. 3. Enlarged view of phase transition region. Note the first-order nature of the transition. The solid line is through the points for to the largest system size. $\beta_Q t=0.083$, $\lambda=10$.

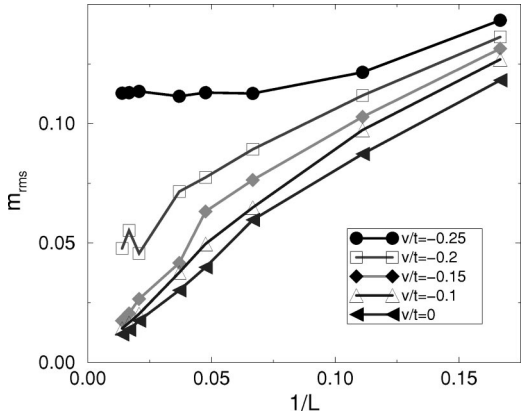

FIG. 4. Scaling of m_{rms} as a function of L^{-1}, the inverse of the linear system size. $\beta_Q t = 0.083$, $\lambda = 10$.

settles down to a nonzero value on the left of the transition, at $v/t = -0.25$, whereas it scales to zero on the right, for $v/t \geqslant -0.15$. The transition is located around $v/t = -0.2$, where the scaling appears inconclusive. From this, we think it is conservative to estimate the transition point between the two phases to be located at $v/t = -0.2 \pm 0.05$.

We conclude this section by addressing potential systematic errors arising from the introduction of the discretization in the stacking direction, since the mapping to the quantum dimer model is exact in the continuum limit only.

In Fig. 5, we show the plots of m_{rms} vs v/t for a system of 2304 sites using different couplings in the stacking direction, K^{τ}, thus varying λ, at a fixed quantum temperature. It can be seen that the transition sharpens up as λ is increased, but moves only little as λ changes from 10 to 20. As the quantum temperature is lowered by a factor of 2 at $\lambda = 20$, the transition sharpens further but again does not move significantly. These effects are therefore certainly within the error bars we give for the value of the critcal v/t. The case of the largest system we have studied (also displayed in Fig. 5) clearly also falls into this range.

We note that the absence of finite-size effects at $v = 0$, upon increasing the number of layers, N, at fixed β_C and L,

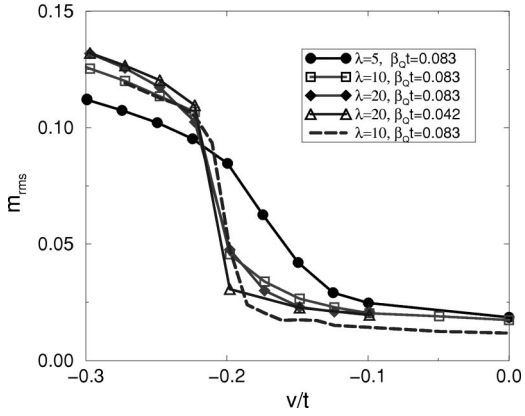

FIG. 5. Development of m_{rms} as a function of λ and β_Q. The dashed line is for 5184 sites; the others are for 2304 sites. Reducing the discretization error (increasing λ) and lowering the quantum temperature (increasing N) sharpen up the transition.

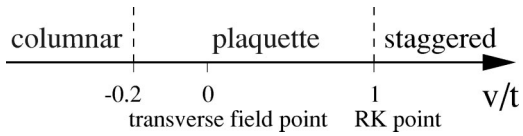

FIG. 6. Phase diagram of the quantum dimer model on the hexagonal lattice. The nature of the ordered phases is indicated above the axis.

implies the existence of a gap in this part of the phase diagram. This is not surprising since at that point, we are far away from the phase transition, which is first order at any rate. However, this observation makes the existence of a gapless excitation at this point, suggested in Ref. 13, seem rather unlikely. More generally, our results fit snugly into the expectations from the height representation analysis as well the analysis of the transverse field Ising models (see below as well) and so there seems little doubt that the analysis in Ref. 13 is flawed.

V. PHASE DIAGRAM

The phase diagram we have thus obtained is depicted in Fig. 6. The columnar-plaquette phase transition is of first order, whereas the one at the RK point is a second-order one, albeit with the somewhat peculiar feature that, coming from the right, it appears to be first order as no fluctuations are visible leading up to the critical point. However, coming from the left, a gap closes, giving rise to the gapless resonon excitations.[1]

There are a number of theoretical reasons which lead us to conclude that the transition from plaquette to columnar VBS is first order, as the simulations suggest. Within the framework of the Landau-Ginzburg-Wilson theory,[15] the critical point corresponds to the vanishing of the coefficent of the sixfold clock term, so that the system could in principle fluctuate between all the degenerate XY states (including the columnar and plaquette ones) without encountering any barriers. However, higher ''harmonics'' (clock terms) will presumably come into play as they are unlikely to vanish at exactly the same point as the leading one; it is these which will prevent the barriers between the plaquette and columnar state from vanishing.

Further, we note that the symmetry groups of the two VBS's are not such that one of them is a subgroup of another, which would be a criterion within Landau theory for a continuous transition. This is in fact a somewhat subtle point as both phases break translational symmetry and retain a sixfold rotational symmetry. However, when trying to form domains of one phase within another, it turns out that the centers of rotational symmetry lie in distinct places for the two phases.

This point, incidentally, is somewhat simpler in the square lattice, where the columnar phase breaks translational symmetry in one direction and also rotational symmetry, whereas the plaquette phase breaks translational symmetry in both directions but retains a fourfold rotational symmetry.

VI. STACKED MAGNETS

Our simulations apply equivalently to the hexagonal dimer model and to the stacked triangular magnets. We

therefore briefly digress here to note some implications of our results to the latter system, on which a good deal of work has been done, in great part inspired by the existence of experimental compounds realizing this model; for a review of both theory and experiment, see Ref. 6.

Recall that H_{Ising} at $v_C=0$ reduces precisely to this model; there, the presence of the plaquette VBS corresponds to the three-sublattice $(+M,0,-M)$ ordering pattern for the triangular magnet. This agrees with the results of Refs. 18–20, whereas it partially disagrees with Refs. 15 and 16.

This result is somewhat surprising, as even in the low-temperature limit it appears that one ends up with only a partially ordered state (spins on one sublattice are still equally likely to point up or down in this phase), rather than the apparently more fully ordered state $(m,-n,-n)$. However, note that in either case, fluctuations are present down to zero temperature—in fact, these states are stabilized by those fluctuations in the first place.[17,5] In the absence of fluctuations, the energy of any ferromagnetically stacked ground-state configuration of the triangular magnet would be the same. Such a selection of an ordered state by fluctuations is known as order by disorder.[29] It has the feature that, although weak fluctuations are needed for stabilizing the state, their strengthening will lead to a melting of the order they themselves established in the first place.

In the present case, it now so happens that the intermediate phase with a disordered sublattice can benefit from the fluctuations and survive them. As fluctuations are suppressed (e.g., by adding a negative v or a magnetic field; see below), one enters the phase with a higher degree of ordering.

We can be reasonably confident that upon lowering the temperature even further, there will not be a transition to the $(m,-n,-n)$, mainly because the critical v/t seems to move very little, if at all, in the right direction, as the temperature is lowered. Nonetheless, we are not entirely clear how to resolve the discrepancies with Refs. 15 and 16. As for the hard-spin mean-field theory,[16] it is conceivable that the fluctuations are somewhat underestimated there, thus landing it on the wrong side of the fine dividing line between the two states. At any rate, we have explicitly simulated temperatures lower than the expected transition temperature and found no transition: for a system of size $27\times27\times1024$ spins at $K^\tau=2.3$ ($\lambda\simeq100$), we find sublattice root-mean-square magnetizations of (0.95,0.12,0.95). The early simulations by Blankschtein *et al.*[15] may have run into problems as ergodicity is lost for single-spin updating at low temperature with an increasing correlation length in the stacking direction,[30] a problem only since remedied with the development of more advanced Monte Carlo simulation technology.[28,31] However, our results are fully consistent with the mean-field analysis of Ref. 15, provided the coefficient of the clock term remains of the same sign throughout the ordered phase.

To illustrate the closeness of the two phases,[16,22] in Fig. 7 we display the sublattice correlation matrix for a system of 2304 spins in a stack of height 120. It can be seen that upon application of a small magnetic field, one leaves the $(+M,0,-M)$ phase and enters the $(m,-n,-n)$ one. Note that in the classical model, the proximity of the phases is artificially enhanced as the strength of the field is effectively multiplied by λ as the correlation length in the stacking direction increases. For this reason, the abscissa of the plot is scaled up by λ.

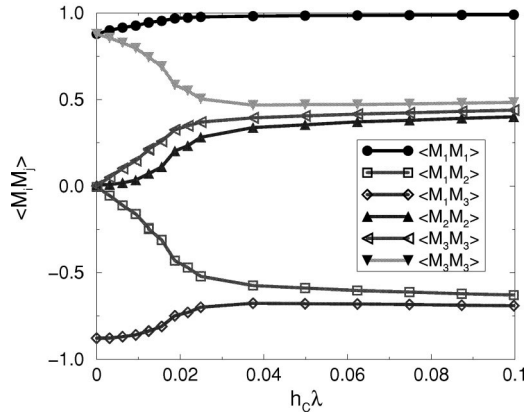

FIG. 7. Correlation matrix of sublattice magnetizations (M_1,M_2,M_3), with $M_1>M_2>M_3$, as a function of magnetic field, for a stack of 120 layers of 2304 sites. $K^\tau=1.15$, so that $\lambda=10$. For $h=0$ one finds the $(+M,0,-M)$ phase, which rapidly gives way to the $(m,-n,-n)$ phase.

VII. RELATION TO THE HEISENBERG ANTIFERROMAGNET

The QDM was conceived to describe the physics of a $S=1/2$ Heisenberg antiferromagnet in a phase dominated by nearest-neighbor singlet bonds (valence bonds or dimers). The question thus arises under what circumstances a VB phase is energetically competitive compared to the Néel state. Note that a spin can form a valence bond with only one of its neighbors, whereas it gains energy from all its anti-aligned neighbors in a Néel state. It is via the resonance moves, captured by $\hat{T}$, that it might make up the energy difference.

One step towards destabilizing the the Néel state is to maximize quantum fluctuations, that is to say, consider spin $S=1/2$ systems. The original idea of Anderson[32] was to choose a frustrated (triangular) magnet, as this does not permit a Néel state in the first place. In addition, in a lattice with low coordination the disadvantage of each spin forming only one VB is relatively less severe, thus favoring a VB state.

Moreover, it is advantageous not to have closed loops which are very short. This can be seen from within the framework of the QDM,[1] which, formally, is an expansion in the overlap between distinct VB configurations. This overlap is exponentially small in the number of VB's in which they differ. The shortest closed loop of even length on the lattice on which the VB's reside determines the lowest-order term in this expansion. This length is 4 for the square and triangular lattice, but 6 for the hexagonal lattice, thus favoring the latter. Furthermore, introducing frustrating further nearest-neighbor exchanges yields a smaller prefactor (but not a smaller expansion parameter) in the RK expansion.

The hexagonal lattice with frustrating further neighbor

exchanges[33] would thus seem to be a good candidate for being described by some sort of QDM. In fact, this expectation appears to be borne out by very recent work of Fouet *et al.*,[23] who did exact diagonalization studies on a J_1-J_2-J_3 $S=1/2$ Heisenberg model on the hexagonal lattice. They indeed found valence-bond phases. For frustrating $J_2/J_1=0.4$, they found a staggered phase, which gives way to a (at least short-range ordered) columnar or plaquette phase around $J_2/J_1=0.3$; the numerics, while not being entirely conclusive, is suggestive of the latter phase.[34]

This is in keeping with the QDM analysis, which indeed suggests that this transition corresponds to crossing the RK point between the plaquette and staggered phases. We should note, however, that carrying out the perturbation theory within the dimer manifold in the spirit of Ref. 1 does not place the point $v=t$ in between those two values of J_2/J_1, and so a more microscopic prediction of the properties of Heisenberg models will probably require going beyond this by including any renormalizations needed to obtain an effective QDM with nearest-neighbor bonds only.

VIII. CONCLUSIONS

We have mapped out the phase diagram of the QDM on the hexagonal lattice. We have established the existence of a plaquette VBS intermediate between a columnar and a staggered one. This was achieved by combining a duality mapping to a classical model with a Monte Carlo cluster algorithm. In the process, we were also able to go well beyond the limitations of previous numerical work on the stacked triangular magnet to confirm the nature of the low-temperature phase in that model. Based on the close connections between the properties of dimer models on the hexagonal and square lattices,[5] we expect the square lattice QDM, which can be obtained from similar simulations on a stacked magnet,[35] to behave in an analogous manner. As detailed in Sec. VII for the hexagonal lattice, this could shed some light on the properties of a J_1-J_2 square lattice Heisenberg model,[36] for which the derivation of the RK model is totally analogous. Nevertheless, the competition between the plaquette and columnar phases is a matter of microscopic detail and so a thorough study of the latter would appear to be in order definitively to settle the issue. We expect to tackle this question in future work.

ACKNOWLEDGMENTS

We would like to acknowledge conversations with J.B. Fouet, C. Henley, D. Huse, C. Lhuillier, S. Sachdev, and P. Sindzingre. The work was supported in part by grants from the Deutsche Forschungsgemeinschaft, NSF Grant No. DMR-9978074, the A. P. Sloan Foundation, and the David and Lucile Packard Foundation.

[1] D. S. Rokhsar and S. A. Kivelson, Phys. Rev. Lett. **61**, 2376 (1998).
[2] S. A. Kivelson, D. S. Rokhsar, and J. P. Sethna, Phys. Rev. B **35**, 8865 (1987).
[3] P. W. Anderson, Science **235**, 1196 (1987).
[4] N. Read and S. Sachdev, Phys. Rev. B **42**, 4568 (1990).
[5] R. Moessner, S. L. Sondhi, and P. Chandra, Phys. Rev. Lett. **84**, 4457 (2000); R. Moessner and S. L. Sondhi, Phys. Rev. B **63**, 224401 (2001).
[6] For a review, see M. F. Collins and O. A. Petrenko, Can. J. Phys. **75**, 605 (1997).
[7] R. Moessner, S. L. Sondhi, and E. Fradkin, cond-mat/0103396 (unpublished).
[8] S. Sachdev, Phys. Rev. B **40**, 5204 (1989).
[9] L. B. Ioffe and I. E. Larkin, Phys. Rev. B **40**, 6941 (1989).
[10] L. S. Levitov, Phys. Rev. Lett. **64**, 92 (1990).
[11] P. W. Leung, K. C. Chiu, and K. J. Runge, Phys. Rev. B **54**, 12 938 (1996).
[12] C. L. Henley, J. Stat. Phys. **89**, 483 (1997).
[13] P. Orland, Phys. Rev. B **47**, 11 280 (1993).
[14] R. Moessner and S. L. Sondhi, Phys. Rev. Lett. **86**, 1881 (2001).
[15] D. Blankschtein, M. Ma, A. N. Berker, G. S. Grest, and C. M. Soukoulis, Phys. Rev. B **29**, 5250 (1984).
[16] R. R. Netz and A. N. Berker, Phys. Rev. B **66**, 377 (1991).
[17] S. N. Coopersmith, Phys. Rev. B **32**, 1584 (1985).
[18] F. Matsubara and S. Inawashiro, J. Phys. Soc. Jpn. **56**, 2666 (1987).
[19] O. Heinonen and R. G. Petschek, Phys. Rev. B **40**, 9052 (1989).
[20] J.-J. Kim, Y. Yamada, and O. Nagai, Phys. Rev. B **41**, 4760 (1990).
[21] A. Bunker, B. D. Gaulin, and C. Kallin, Phys. Rev. B **48**, 15 861 (1993).
[22] M. L. Plumer and A. Mailhot, Physica A **222**, 437 (1995).
[23] J. B. Fouet, P. Sindzingre, and C. Lhuillier, Eur. Phys. J. B **20**, 241 (2001).
[24] A. Kekule, Bull. Soc. Chim. Fr. **3**, 98 (1865); L. Pauling, Proc. Natl. Acad. Sci. U.S.A. **39**, 551 (1953).
[25] C. L. Henley (unpublished); for a brief review of the argument, see Ref. 7.
[26] This mapping is based on the duality of an Ising model and an Ising gauge theory in $d=2+1$ [for a review, see R. Savit, Rev. Mod. Phys. **52**, 453 (1980)]. The ground states of the two models are guaranteed to coincide, whereas the lowest excited state may reside in a sector not captured by the duality transformation. For details, see Refs. 5 and 7.
[27] In fact, the naive LGW treatment gives $n=m/2$ and hence both patterns with zero magnetization. However, for the $(+M,0,-M)$ but not for the $(+m,-n,-n)$ pattern, this property is protected by the sublattice symmetry, so that generically $n\neq m/2$. We have explicitly checked in our numerics that the Ising symmetry breaking transition is indeed the one between these two patterns.
[28] R. H. Swendsen, J. S. Wang, and A. M. Ferrenberg, Top. Appl. Phys. **71**, 75 (1992). For a didactic review, see W. Krauth, in *Advances in Computer Simulation*, edited by J. Kertesz and I. Kondor (Springer-Verlag, Berlin, 1998).

[29] J. Villain, R. Bidaux, J. P. Carton, and R. J. Conte, J. Phys. (Paris) **41**, 1263 (1980); for a review, see R. Moessner, Can. J. Phys. (to be published).

[30] Note, also, that the microscopic parameters used in the simulations are not exactly the same. In our simulation, we took the limit of infinite spatial coupling.

[31] In fact, Ref. 20 already employed a cluster algorithm. There, however, system sizes were used which were so small that at low temperature, the correlation length in the stacking direction was larger than the system size. In this limit, one is effectively simulating a classical monolayer system or, alternatively, the *high-temperature* limit.

[32] P. W. Anderson, Mater. Res. Bull. **8**, 153 (1973); P. Fazekas and P. W. Anderson, Philos. Mag. **30**, 23 (1974).

[33] For previous work, see A. Mattsson, P. Frojdh, and T. Einarsson, Phys. Rev. B **49**, 3997 (1994) and references therein.

[34] J. B. Fouet (private communication).

[35] R. A. Jalabert and S. Sachdev, Phys. Rev. B **44**, 686 (1991).

[36] V. N. Kotov, M. E. Zhitomirsky, and O. P. Sushkov, Phys. Rev. B **63**, 064412 (2001) and references therein.